A Thesis for the Degree of Master of Science

GC MS-Based Metabolomic Approach to Understand the Mucin Utilization of *Vibrio vulnificus*

GC-MS 기반의 대사체학적 접근을 통한 패혈증 비브리오균의 Mucin 이용에 대한 이해

February, 2014

Sun Haeng Jang

Department of Agricultural Biotechnology
College of Agriculture and Life Sciences
Seoul National University

석사학위논문

GC MS-Based Metabolomic Approach to Understand the Mucin Utilization of *Vibrio vulnificus*

지도교수 최 상 호

이 논문을 석사학위논문으로 제출함

2014 년 2 월

서울대학교 대학원

농생명공학부

장 선 행

장선행의 석사학위논문을 인준함

2014 년 2 월

위원장 장 판 식 (인)

부위원장 최 상 호 (인)

위원 이 기 원 (인)

Abstract

Mucin, a highly glycosylated large glycoprotein, is a major component of mucus layer in the human body and could serve as a source of nutrient to support the growth of enteropathogens. To gain insight into the metabolisms used by human enteropathogen *Vibrio vulnificus* to utilize mucin, the metabolic profiles of *V. vulnificus* in the media containing mucin and glucose were compared for *in vitro* analysis. Also, *V. vulnificus* infecting to HT29-MTX mucin secreting cell line and medium control were compared for *ex vivo* analysis. For *ex vivo* experiment, mucin secreting cell line was constructed and confirmed whether it secretes mucin or not by transmission electron microscopy (TEM), scanning electron microscopy (SEM), and confocal laser scanning microscope (CLSM). The global metabolite profiling was conducted by using gas chromatography-time of flight mass spectrometry (GC-TOF-MS) and in-house programmed database and standards. In the *in vitro* experiment, principal component analysis revealed clear separations between the intracellular metabolite profiles of *V. vulnificus* utilizing mucin. When *V. vulnificus* grown with mucin, both the level of N-Acetyl-D-mannosamine-6-phosphate and N-Acetylglucosamine-6-phosphate a catabolic intermediate of N-acetylneuraminic acid (Neu5Ac) which is a terminal carbohydrate of mucin were increased. The level of amino acids, fatty acids and pyruvate were increased in the mucin utilizing cells both *in vitro* and *ex vivo* metabolomics analysis. Taken together, the use of mucin as a nutrient source in *V. vulnificus* led to the increase abundances of amino acids,

fatty acids, sialic acid, and TCA cycle intermediates by activating the catabolic pathways.

Key words: *Vibrio vulnificus*, Mucin, Metabolomics, GC-TOF-MS

Student Number: 2012-21178

Contents

Abstract……i

Contents……iii

List of Figures……v

List of Tables……vi

I. INTRODUCTION……...1

II. MATERIALS AND METHODS……...4

Strain and culture condition ……..……4

In vitro bacterial cell culture…….. 4

Cold methanol quenching (*in vitro* sample preparation) ……4

Metabolites extraction……5

Derivatization of metabolites.....…….……..……6

GC-TOF-MS analysis.....……..……...…6

Data processing ……..7

Statistical analysis...……7

Construction of HT29-MTX cell line……8

Transmission electron microscopy (TEM).…….……...8

Scanning electron microscopy (SEM) …..…….....9

Immunofluroscence staining analysis …..……. ……...10

HT29-MTX cell culture and infection with *V. vulnificus*……11

Fast filtration (*ex vivo* sample preparation) …… 11

III. RESULT……14

Bacterial cell growth profile in the mucin supplemented media ……14

Schematic flow of sampling procedures of cold methanol quenching and extractio n.……16

In vitro, multivariate analysis of metabolites profiles……..18

Comparison of metabolites abundances on the mucin……..20

Sialic acid metabolism pathway analysis……..25

Construction of the mucin-secreting HT29-MTX cells and microscopic assays for confirmations…….27

Survival assay of *V. vulnificus* infecting HT 29-MTX cell line…….……..31

Schematic flow of sampling procedures of fast filtration…….33

Ex vivo, multivariate analysis of metabolites profiles……..35

Comparison of metabolites abundances on the infecting *V. vulnificus*…….37

Analysis of fatty acid metabolism pathway in *V. vulnificus*……..41

IV. DISCUSSION…….…43

V. REFERENCES…….48

VI. 국문초록……52

List of Figures

Fig. 1. Growth of *V. vulnificus*……..15

Fig. 2. Schematic flow of *in vitro* sample preparation ……17

Fig. 3. *In vitro* analysis PCA score plot and PLS-DA score plot…….19

Fig. 4. Clustered heat map of *in vitro* analysis……..21

Fig. 5. Metabolic pathway of sialic acid (Neu5Ac) in *V. vulnificus* and box-whisker plots……..26

Fig. 6. Microscopic analysis of secreted gel-forming mucin by HT29-MTX cell line……28

Fig. 7. Survival curve of *V. vulnificus* infecting HT29-MTX……..32

Fig. 8. Schematic flow of *ex vivo* sample preparation…….34

Fig. 9. *Ex vivo* analysis PLS-DA score plot…….36

Fig. 10. Clustered heat map of *ex vivo* analysis……...38

Fig. 11. Metabolic pathway of fatty acid in *V. vulnificus*……41

List of Tables

Table 1. Bacterial strains and plasmids used in this study……13

Table 2. The most significantly different metabolites identified in the *V. vulnificus* grown with mucin (M9M) relative to the glucose (M9G)..……. 22

Table 3. The most significantly different metabolites identified in the *V. vulnificus* infecting mucin secreting HT29-MTX cell line relative to growing in the medium control..……..…….39

I. INTRODUCTION

Vibrio vulnificus is a Gram-negative, motile, curved rod-shaped bacterium with a single polar flagellum. Like other organisms in *Vibrionaceae*, *V. vulnificus* is a facultative anaerobe having the ability of fermentation. It causes an invasive septicemia usually contracted through the consumption of raw or undercooked shellfish, as well as wound infections (Storm and Parajpye, 2000; Gulig *et al*., 2005). The mortality of primary septicemia caused by *V. vulnificus* is very high (>50%) and death can occur within one to two days after the first signs of illness (Linkous and Oliver, 1999; Melissa and Oliver, 2009).

In the host, *V. vulnificus* moves via gastrointestinal tract and reaches the human intestinal epithelial cells that are covered with mucus layer where bacteria primarily colonize on (McGuckin *et al*., 2011). The mucus layer which is a viscous, highly hydrated fluid layer consists of water, salts, lipids and proteins, even though the main component of mucus layer is mucin. Mucin is a complex and high-molecular-weight glycoproteins characterized by the presence of a large theronine and/or serine-rich tandem repeated domain which is rich in complex o-linked oligosaccharides (Allen, 1981; Rose, 1992; McGuckin *et al*., 2011).

When bacteria invade the human gut, adverse environmental changes, such as increased competition for the specific nutrients imposed by the host cells and

endogenous commensals, are encountered. Thus, the ability acquire and metabolize those nutrients is crucial for bacteria to survive and multiply in the intestine (Chang *et al*., 2004; Brown *et al*., 2008). In the intestine, as the glucose limited condition, enteropathogenic bacteria must be able to use alternative nutrients to achieve a successful infection (Lang *et al*., 1994). In this aspect, utilization ability of mucus components is very important survival factors to enteropathogens.

Metabolomics, which involves the comparative and non-targeted analysis of the complete set of metabolites in a cell, enables a global view of cellular functions since the metabolome directly reflects the physiological status of a cell (Mashego *et al*., 2007; Pope *et al*., 2007; van der Werf *et al*., 2008). The key assumption of metabolomics is that differences in the metabolic composition of samples reflecting differences in physiological states can be detected and studied (Fiehn, 2002). Metabolome analysis covers the identification and quantification of all intracellular and extracellular metabolites with molecular mass lower than 1000 Da, using different analytical techniques. In addition to applications in functional genomics, quantification of metabolite concentrations enables identification of the kinetics that underlies specific intracellular reactions (Buchholz *et al*., 2002; Hellerstein, 2004).

Several studies have used the metabolomics approach to discover new and informative metabolites in the biological systems. Consequently, range of analytical platforms, such as nuclear magnetic resonance (NMR), gas chromatography–mass spectrometry (GC–MS), capillary electrophoresis mass spectrometry (CE–MS), and

liquid chromatography mass spectrometry (LC–MS), were developed (Dunn *et al*., 2005). Recent technological advances in mass spectrometry have realized reliable and highly sensitive measurements of metabolites (Villas-Bôas *et al*., 2006). Among them, gas chromatography mass spectrometry (GC–MS) has been successfully applied to analyze and interpret multiparametric metabolic responses in living systems to pathophysiological and environmental perturbations (Scherling et al., 2010). To gain a better understanding of the metabolic pathway in *V. vulnificus*, it would be useful to investigate the metabolic changes of the *V. vulnificus* when utilizing mucin both *in vitro* and *ex vivo* conditions.

In this study, I investigated the metabolic profiles and metabolism of *V. vulnificus* grown in minimal media supplemented with mucin powder as a sole carbon source. Also, I explored the metabolic changes of *V. vulnificus* when infected to mucin secreting cell line, HT29-MTX. To accomplish these, I used metabolomics with gas chromatography-time of flight mass spectrometry (GC-TOF MS) and multivariate statistical analyses to identify biomolecular changes. Then I evaluated the metabolic patterns associated with utilization of mucin.

II. MATERIALS AND METHODS

Strain and culture condition. The strain used in this study is listed in Table 1. Unless otherwise noted, *V. vulnificus* strain was grown in Luria-Bertani (LB) medium supplemented with 2.0% (wt/vol) NaCl (LBS) at 30℃. When required, M9 (Sambrook and Russell, 2011), in which one of the carbon sources such as mucin (0.9%, wt/vol) or glucose (0.4%, wt/vol) was supplemented, was used as a minimal medium. The pig gastric mucin powder was used and sterilized with 95%(w/v) ethanol (Mitsui, *et al*., 1976). All the media components were purchased from Difco (Detroit, MI), and the chemicals were purchased from Sigma (St. Louis, MO).

***In vitro* bacterial cell culture.** Freshly streaked colony was inoculated in M9 supplemented with glucose (0.4%, wt/vol) and cultured 12 hours at 30℃. 1 ml of culture was washed by 1ml of M9 base and cell pellets were resuspended with 1ml of M9 base. 500 μl of resuspended cells was used to inoculate a 50 ml subculture in M9 supplemented with mucin (0.9%, wt/vol) or glucose (0.4%, wt/vol) respectively. All cultures were incubated at 30℃ with shaking (250 rpm).

Cold methanol quenching (*in viro* sample preparation). *V. vulnificus* cells grown to early-, mid-, late-log, and stationary phases were harvested and quenched with cold methanol. Part of the cell suspension was transferred to a 50 ml falcon tube (BD, San jose, CA, USA) containing the same volume of precooled (−70℃) 70%

(vol/vol) methanol solution with 0.07 M HEPES buffer (pH 7.5) (Mashego *et al.*, 2007, Shin *et al.*, 2010a). Each culture volume was determined by the volume containing 1×10^{10} cfu of bacteria.

The suspension was inverted mildly for 2 times. After centrifugation at 4000 g, 4℃ for 15 minutes, the resulting pellets were washed in cold (4℃) 10 ml of 0.9% (w/v) sodium chloride (NaCl) solution. The centrifugation was repeated after washing step for 10 minutes. The cells were resuspended in 4℃, 1 ml of 0.9% (w/v) NaCl solution and transferred to the eppendorf tube (Eppendorf, Hamburg, Germany). The centrifugation was repeated after second washing step for 10 minutes (Marcinowska *et al.*, 2011). Collected quenched cell pellets were vacuum dried for 10 hours prior to cell disruption and dried bacterial pellets were kept at -80℃ until extraction.

Metabolites extraction. A zirconium carbide bead (diameter, 5mm) was added to the tube containing dried pellet then agitated it using a MM301 mixer mill (Retsch, Haan, Germany) at a frequency of 30 Hz for 3 minutes (Marcinowska *et al*., 2011). The disrupted cells were then extracted with 1 ml of extraction solvent, mixture of acetonitrile / methanol / water (Gibco, NY, USA) (AMW; 2:2:1, v/v/v) at 4℃ (Shin *et al.*, 2010b) and agitated it at 30 Hz for 2 minutes. After centrifugation at 15000 rpm, 2℃ for 10 minutes, the extracts were transferred to the eppendorf tube and concentrated to dryness in a vacuum concentrator (Biotron, Seoul, Korea).

Derivatization of metabolites. Prior to GC-TOF-MS analysis, dried metabolites were derivatized by methoxyamination and silylation. Briefly, 50 µl of 20 mg/ml methoxyamine hydrochloride in pyridine was added to metabolite samples and incubated for 90 minutes at 30 ℃ in the thermo mixer (Eppendorf, Hamburg, Germany). The metabolites samples were then mixed with 45 µL of *N*-methyl-*N*-trimethylsilyltrifluoroacetamide (MSTFA) and incubated for 30 minutes at 37℃ (kim *et al*., 2013). The derivatized metabolites were transferred to GC vial.

GC-TOF-MS analysis. The derivatized metabolite samples were analyzed by GC-TOF-MS using an Agilent 7890A gas chromatography (Agilent Technologies, Wilmington, DE) coupled with a Pegasus III TOF MS (LECO, St. Joseph, MI). Each sample (1 µl) was injected by an autosampler (Agilent 7693) equipped with a Rtx-5MS capillary column (30 m length × 0.25 mm i.d. × 0.25 µM film thickness-Agilent J&W GC column) in splitless mode. Helium was used as the carrier gas at a constant flow rate of 1.5 ml/minutes. The injector temperature was 250 ℃, and the injection volume was 1 µl. The oven temperature program commenced from 75 ℃ for 2 minutes, followed by 300 ℃ from 2 to 15 minutes, with a 15 ℃/minute hold, and finally a hold of 3 minutes, with a transfer line temperature of 240 ℃.

In MS, ionization was at − 70 V (electron energy) with a source temperature of 230 ℃. The detector voltage was 1450 V, and the mass range was set at 45–800 m/z with an acquisition rate of 10 spectra per second.

Data processing. GC-TOF-MS raw data files were converted to computable document format (*.cdf) by the inbuilt data processing software of the Agilent GC system programs. After obtaining the CDF format, the files were subjected to preprocessing, peak extraction, retention time correction and alignment using metAlign software package (http://www.metalign.nl). After analysis, the resulting peak list was obtained as a .txt file, which was later exported to Microsoft Excel (Microsoft, Redmond, WA, USA). The Excel file contained the corrected peak retention time, peak area and corresponding mass (m/z) data matrix for further analysis. The acquired data were normalized to the total cell number determined by CFU prior to analyze by multivariate data modeling.

Statistical analysis. SIMCA-P software 12.0 (Umetrics, Umeå, Sweden) was used for principle component analysis (PCA). Partial least-squares discriminate analysis (PLS-DA) was carried out using auto-scaled and log-transformed data to identify the metabolites showed variation between control and mucin samples. Based on the variable importance in projection (VIP) values (> 0.7) and a threshold of < 0.05 for Student's t-test of individual samples, the variable selection was made and compared by box-and-whisker plots using STATISTICA (version 7.0; StatSoft Inc., Tulsa, OK, USA). Annotation of peaks were based on standard retention times, m/z, and existing references.

Construction of cell line HT29-MTX. Human colon carcinoma epithelial cell lines, HT-29 cells, were purchased from American Type Culture Collection (ATCC, Manassas, VA) and maintained in McFP medium [McCoy's 5A medium supplemented with 10% fetal bovine serum (FBS) (PAA, Pasching, Austria) and antibiotics (1% (w/v) penicillin/streptomycin)]. HT-29 cells were grown in 75cm^2 culture flask (SPL, Kyungki, Korea) at 37℃ in the 5% CO_2 incubator. For differentiation, HT-29 cells were prepared by seeding 1×10^6 cells in 9 ml of culture medium in 25 cm^2 culture flask (SPL, Kyungki, Korea) and added the 18 μl of 5×10^{-4} M methotrexte(MTX) diluted in 37℃ pre-warmed phosphate-buffered saline (PBS). The medium was changed daily in all culture conditions. After weekly passages, the HT-29 cells which survived in the presence of 1×10^{-6} M MTX are called HT29-MTX (Lesuffleur *et al*., 1990).

Transmission electron microscopy (TEM). 10 days incubated HT-29 and HT29-MTX cells were treated with Trypsin-EDTA for 10 minutes at 37℃ and detached from 75cm^2 culture flask. The cells were resuspended with modified Karnovsky's fixation solution [2% (w/v) paraformaldehyde and 2% (w/v) glutaraldehyde in 0.05 M sodium cacodylate buffer (pH 7.2)] and incubated at 4℃ for 3 hours. The samples were washed with 0.05 M sodium cacodylate buffer and stored at 4℃ for 10 minutes. After centrifugation at 1000 rpm for 3 minutes, repeated washing step 3 times. For post fixation, treated with 1% (w/v) osmium tetroxide in 0.05 M sodium cacodylate buffer at 4℃ for 2 hours. The samples were rinsed with water 2 times and incubated with 0.5% (w/v) uranyl acetate for 30 minutes at 4℃. The samples

were dehydrated with 30, 50, 70, 80, 80, 100% (v/v) alcohol. Treated with each concentration of alcohol for 10 minutes and repeated 3 times for 100% alcohol. Then incubated sample with propylene oxide for 15 minutes. The samples were shacked with 1:1 mixture of propylene oxide and spurr's resin [10g of ERL 4221 (vinyl cyclohexane dioxide), 6g DER 736 (diglycidyl ether of polypropylene glycol), 26g NSA (nonenyl succinic anhydride), 0.4g DMAE (dimethylaminoethanol)] for 2 hours. Then shacked sample with the 1.5 ml spurr's resin for overnight and replaced with new spurr's resin shacking for 2 hours. The sample was incubated for 24 hours at 70℃ and sectioned the embedded cells by ultramicrotome (MTX, RMC, USA). The sectioned cells were observed with transmission electron microscopy (JEM1010, JEOL, Japan) (Lesuffleur *et al.*, 1990).

Scanning electron microscopy (SEM) HT29-MTX cells were seeded on 12-mm diameter polycarbonate filter inserts (Transwell® , Corning, MA, USA) at a density of 2×10^5 cells per filter. Cells were incubated at 37℃ in the 5% CO_2 incubator and the culture medium was changed every day for 30 days, during which time the cells had reached confluency (Pontier *et al.*, 2008).

Cells were fixed with 2% (v/v) glutaraldehyde and 2% (v/v) paraformaldehyde in 0.05 M cacodylate buffer (pH 7.2) at 4℃ for 2 hours. Fixed cells were washed 3 times with 0.05 M cacodylate buffer (pH 7.2) at 4℃ mildly. Then the cells were post fixed in 1% osmium tetroxide (OsO_4) in 0.05 M cacodylate buffer (pH 7.2) at 4℃ for 2 hours and wash with distilled water briefly. The cells were dehydrated through graded ethanols, 30 to 100%, critical point dried with 100%

Hexamethyldisilazane (HMDS), and mounted the cell grown membrane on the metal stub. Mounted cells were gold coated by sputtering (SCD 005, Bal-Tec, Switzerland) (Donelli et al., 1996). The samples were examined with a field-emission scanning electronic microscopy (Augira, Carl Zeiss, Germany).

Immunofluroscence staining analysis. HT29-MTX cells were grown for 6 days on the circle-shaped cover glass (diameter, 1 cm) mildly attached on the 12-well microtiter plate (SPL, Korea). Transferred the cell grown cover glass to the new 12-well microtiter plate and washed with PBS mildly. The cells were fixed with 1 ml of 3.5% (w/v) para-formaldehyde for 10 minutes and washed with PBS twice. Incubated with 0.1% Triton X-100 with PBS and rinsed with PBS. Treated with blocking solution [1% (w/v) FBS in PBS (FPBS)] for overnight at 4℃.

Removed the FPBS and transferred the cell grown cover glass to the parafilm. After washed with PBS, treated with the 1/100 diluted mouse monoclonal antibodies (Merck millipore, Darmstadt, Germany) against human MUC5AC protein in PBS for 1 hour at room temperature (Vieira *et al*., 2010).

The cells were rinsed and incubated with rabbit anti-mouse IgG-FITC secondary antibodies (Abcam, Cambridge, UK) in PBS for 1hour at room temperature without light. Removed the antibodies and the cell grown cover glass was transferred to the slide glass.

Then treated with DAPI (4',6-diamidino-2-phenylindole) containing mounting solution (Vector, CA, USA) and sealed the surround of cover glass with nail polish to prevent drying and movement under microscope.

The confocal laser scanning microscope (CLSM) (Carl Zeiss LSM710, Germany) was used to observe the stained HT29-MTX cells (Gouyer *et al.*, 2001). The images were reconstructed using Zen software (Carl Zeiss, Oberkochen, Germany).

HT29-MTX cell culture and infection with *V. vulnificus*. The 3×10^6 HT29-MTX cells were seeded in under part of polycarbonate membrane transwell culture plate (Transwell® , Corning, MA, USA) and incubated at 37℃ in the 5% CO_2 incubator. The McFP medium was changed every day for 10 days, during which time the cells had reached over confluency at 1×10^8 cells. Then infected with *V. vulnificus* strains at an MOI of 20 using basal medium eagle (BME) medium and incubated at 37℃ in the 5% CO_2 incubator. After each 1, 2 and 3 hours infection, collected infecting *V. vulnificus* which were in inner part of the membrane insert.

Fast filtration (*ex vivo* sample preparation). The 9 mL of infecting bacterial sample were vacuum-filtered through isopore membrane filter (0.4 μm pore size, 47 mm diameter; Merck, Billerica, MA, USA) and washed with 10 ml of 0.9% (w/v) NaCl solution. Both the filtered cell mass and the used filter were quickly mixed with 2 ml of a metabolite extraction solvent the 4℃ mixture of AMW. The entire procedure including fast filtration to membrane transfer was completed within 1 minute. The dish was sonicated for 5 minutes at 4℃ waterbath sonicator and stirred for 15 minutes to suspend the cells and extract completely. A 1.9 ml (0.95 ml × 2) portion of the AMW cell suspension was transferred to 1.75ml eppendorf tubes and

centrifuged at 4000 g and 4 ℃ for 10 minutes. The extracts (supernatants) were transferred to 1.75ml eppendorf tubes and vacuum-dried. (Ohashi *et al.*, 2008). The extracts were resuspended in 300 μL of fresh acetonitrile/water mixture (1:1, v/v) (50ACN) at 4 ℃ to eliminate lipids and wax and collected together to weighed eppendorf tube. Then, concentrated to dryness in a vacuum concentrator and weighed the eppendorf tube containing dried metabolites (Shin *et al.*, 2010).

Table 1. Bacterial strains used in this study.

Strain or plasmid	Relevant characteristics [a]	Reference or source
Bacterial strains		
V. vulnificus		
MO6-24/O	wild type *V. vulnificus*, virulent	Laboratory collection

III. RESULTS

Bacterial cell growth profile in the mucin supplemented media.

To investigate whether wildtype *V. vulnificus* can utilize mucin or not and at that time of growth phase, *V. vulnificus* was grown in M9 minimal with mucin as the sole carbon source. Also, to obtain the similar growth profiles when *V. vulnificus* utilize glucose and mucin as the sole carbon source, colony forming unit was counted at each conditions. It was found that *V. vulnificus* grown in the 0.4% (v/v) glucose (M9G) and 0.9% (v/v) mucin (M9M) medium represented similar growth phases (Fig. 1). From this result, the possibility of utilization of mucin by *V. vulnificus* and the concentration of two carbon sources, glucose and mucin, giving similar *V. vulnificus* growth profiles were confirmed.

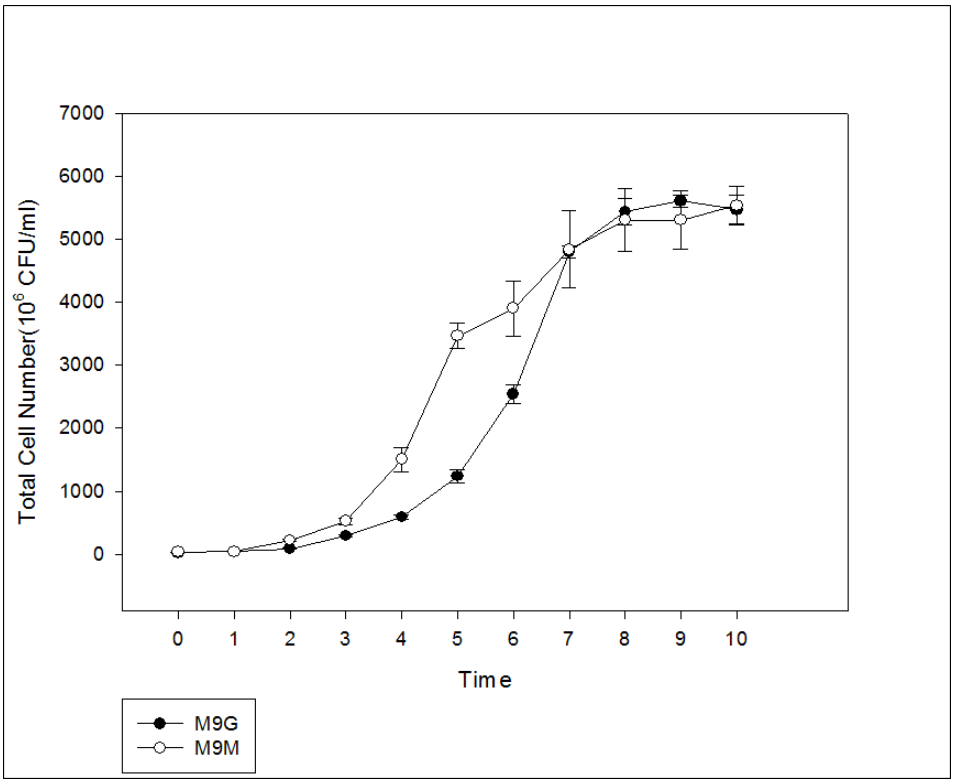

Fig. 1. Growth of *V. vulnificus*. *V. vulnificus* cells grown overnight (during 12hrs) in M9 minimal medium supplemented with 0.4% glucose (M9G) were inoculated in the M9G and in M9 media supplemented with 0.9% mucin (M9M) respectively. Flasks were shaken at 30℃ and 250 rpm, and aliquots were withdrawn every hour and serially plated onto LBS agar plates. Then incubated in 30℃ incubator for 12 hours and colonies were counted.

Schematic flow of sampling procedures of cold methanol quenching and extraction.

Metabolome sampling is one of the most important factors that determine the quality of metabolomics data. The methods for quenching and extraction are undoubtedly sample- and cell-dependent; differences in cellular composition (especially cell membrane and cell wall structure) and cell size may influence the efficiency of quenching and the rate of metabolite leakage.

The main steps in metabolite sample preparation include quenching and metabolite extraction (Kim *et al*., 2013). Many metabolites are very labile and have high turnover rates. Thus, to generate an authentic profile of a system's metabolic composition cellular metabolism should first be stopped (quenched). The most widely used quenching method is to add cold methanol, prior to collecting cells by centrifugation. Adding salts, such as ammonium bicarbonate, HEPES, or NaCl has been shown to help protect cells from breakage, giving a better recovery of metabolites (Sellick *et al*., 2009).

After quenching and washing, the metabolites need to be extracted, which requires disruption of the cell membrane. Cell breakage methods can be chemical or mechanical, the latter involving application of pressure and/or shearing forces of some kind. (Marcinowska *et al*., 2011). Several different extraction methods and solvents have been reported. Several organic solvent mixtures have been applied to bacteria, especially acetonitrile / methanol/ water mixture (AMW; 2:2:1) was applied to gram negative bacteria, *sacchaophagus degradans* and revealed high extraction efficiency (Shin *et al*., 2010b).

In this experiment, precooled (−70℃) 70% (vol/vol) methanol solution with 0.07 M HEPES buffer (pH 7.5) was used for quenching and cold (4℃) 10 ml of 0.9% (w/v) sodium chloride (NaCl) solution was used for washing solution. Also, the composition and condition of extraction solvent is mixture of acetonitrile / methanol / water (Gibco, NY, USA) (AMW; 2:2:1, v/v/v) at 4℃ and physically forced by bead milling (Fig. 2)

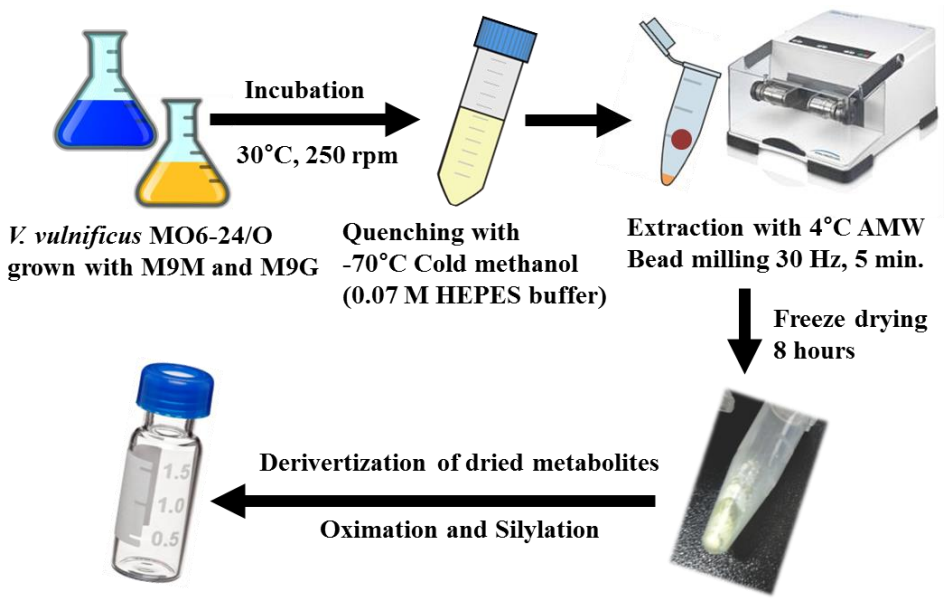

Fig. 2. Schematic flow of *in vitro* sample preparation. The incubated cultures were quenched by 70% (vol/vol) methanol solution at 70℃, and the metabolites were extracted in AMW at 4℃ by bead milling. Extracted metabolites were concentrated to dryness; following dried metabolites were derivatized by methoxyamination and silylation.

***In vitro*, multivariate analysis of metabolites profiles.**

A total of 24 samples from 8 different classes in the three biological replicates and two analytical replicates were analyzed during the early, mid, late -exponential phases and the stationary phase. Metabolites from all major pathways, including TCA cycle intermediates, lipids, sugars, and amino acids were detected. To provide comparative interpretations of the changes in metabolic profiles, principal component analysis (PCA) for unsupervised evaluation and partial least squares discriminant analysis (PLS-DA) for supervised evaluation (independent t-tests) were used to evaluate the mass spectral data of the metabolome from *V. vulnificus* grown in different carbon sources; mucin and glucose during the four growth phases. As shown in Figure 3 A, the PCA results demonstrated that the third principal component (PC 3) differed significantly when different carbon sources were used. In the PLS-DA analysis, vectors t[1] and t[2] explained 25.7% and 17.8% of the variation between mucin and glucose utilizing samples (Fig. 3 B). PLS-DA analysis revealed a clear separation of *V. vulnificus* utilizing mucin and glucose.

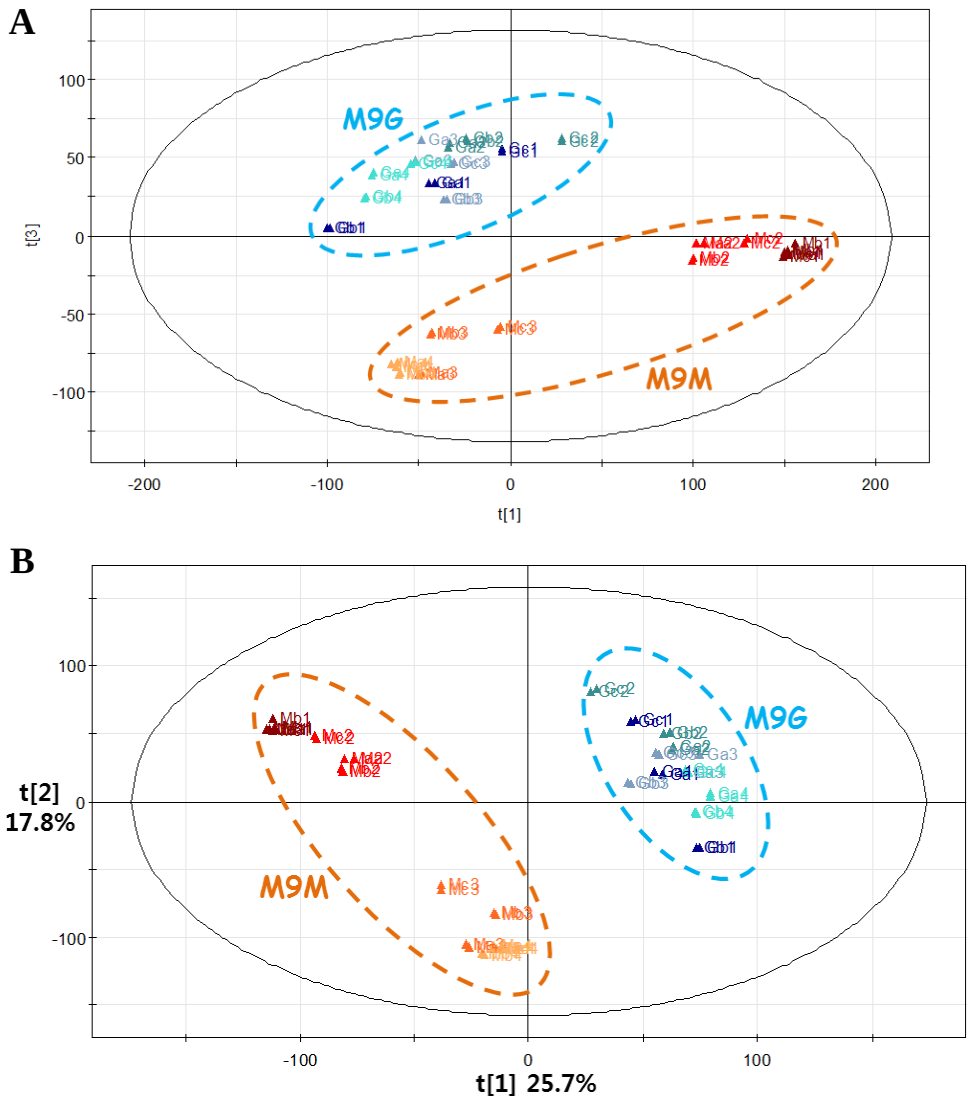

Fig. 3. *In vitro* analysis PCA score plot and PLS-DA score plot. These plots were derived from GC-TOF-MS data sets analyzing *V. vulnificus* metabolism grown with mucin and glucose media. These plots explained that the result of *V. vulnificus* metabolism grown with mucin (M9M) is different from the metabolism grown with glucose media (M9G).

Comparison of metabolites abundances on the mucin.

The metabolites reflecting variation between the *V.vulnificus* grown in the M9G and M9M were identified based on the VIP (variable importance of the projection) and *p*-values. The identified metabolites were annotated based on their retention time in comparison with standards and their mass fragmentation (Table 2). A total of 50 primary metabolites, including 13 lipid related compounds, 8 amine related compounds, 17 amino acids, 8 sugars and 4 organic acids showed significant variation among the samples (Fig. 4).

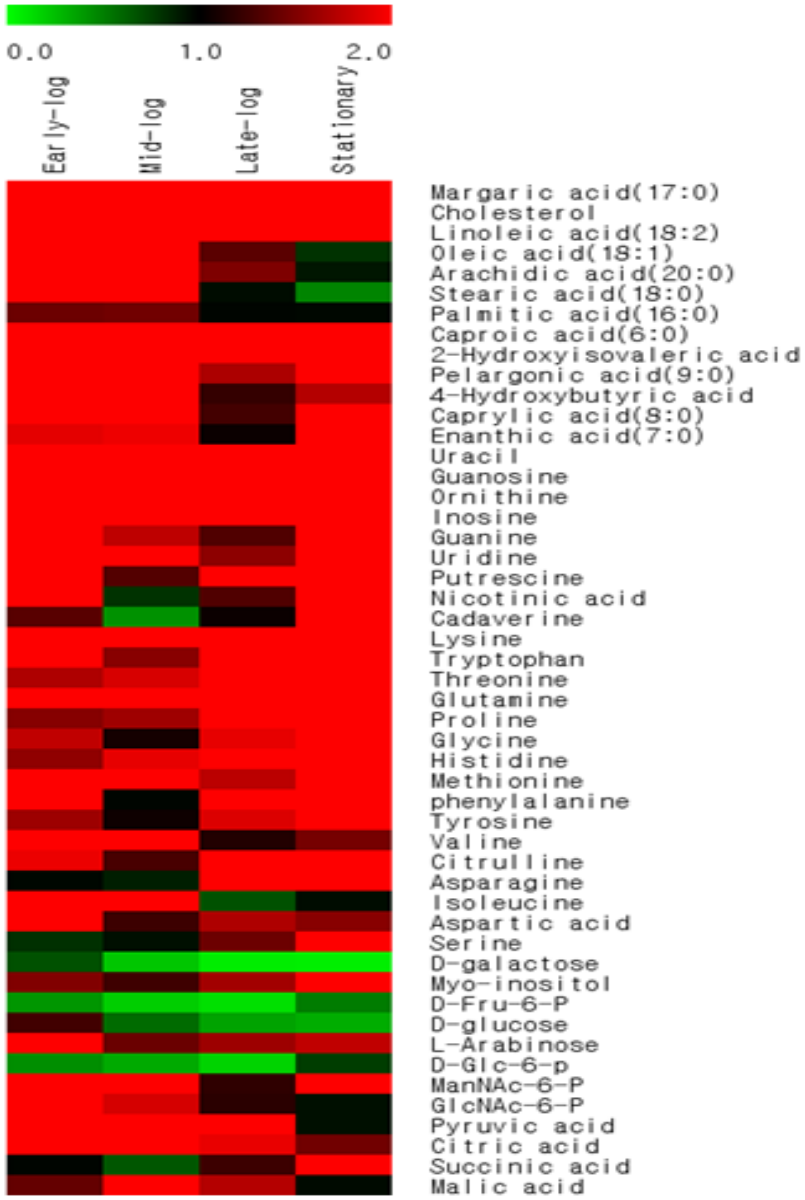

Fig. 4. Clustered heat map of *in vitro* analysis. Significantly different intracellular metabolites between *V. vulnificus* grown with mucin(M9M) and glucose(M9G) during four growth phases. The number stands for the fold change ratio of M9M:M9G. (Variable selection: VIP value >0.7 and *p*-value <0.05)

Table 2. The most significantly different metabolites identified in the *V. vulnificus* grown with mucin (M9M) relative to the glucose (M9G)

RT[a](min)	MS fragmentation[b] (m/z)	Compound[c]	Derivatized[d]	ID[e]
5.04	**45,31,75,117,145,173**	**Caproic acid(6:0)**	**TMSi(X1)**	**MS**
5.93	**47,73,75,117,127,147,232**	**4-Hydroxybutyric acid**	**TMSi(X2)**	**MS**
5.98	**45,73,75,117,129,131,132,145,187**	**Enanthic acid(7:0)**	**TMSi(X1)**	**MS**
5.99	**47,73,75,145,147,219,247**	**2-Hydroxyisovaleric acid**	**TMSi(X2)**	**MS**
6.51	**45,73,100,144,218,246,326,362**	**Valine**	**TMSi(X2)**	**MS/STD**
6.92	**75,11,117,173,201,289,332,360,412**	**Caprylic acid(8:0)**	**TMSi(X1)**	**MS/STD**
7.25	**51,78,90,106,117,136,180,195**	**Nicotinic acid**	**TMSi(X1)**	**MS/STD**
7.26	**45,73,100,158,218,260,318,374**	**Isoleucine**	**TMSi(X2)**	**MS/STD**
7.30	**45,59,73,84,100,133,142,216**	**Proline**	**TMSi(X2)**	**MS/STD**
7.39	**45,73,86,117,147,174,248,276,357**	**Glycine**	**TMSi(X3)**	**MS/STD**
7.41	**45,55,73,86,129,147,172,218,247**	**Succinic acid**	**TMSi(X2)**	**MS/STD**
7.68	**45,73,85,99,113,147,169,241**	**Uracil**	**TMSi(X2)**	**MS/STD**
7.81	**45,75,105,117,145,215**	**Pelargonic acid(9:0)**	**TMSi(X1)**	**MS**
7.88	**45,73,147,174,204,278,306,364**	**Serine**	**TMSi(X3)**	**MS/STD**
8.13	**45,73,86,117,147,219,248,291,350**	**Threonine**	**TMSi(X3)**	**MS/STD**
8.99	**45,73,147,189,233,335,376**	**Malic acid**	**TMSi(X3)**	**MS/STD**
9.25	**73,128,176,219,293**	**Methionine**	**TMSi(X2)**	**MS/STD**
9.25	**73,147,232,294,334**	**Aspartic acid**	**TMSi(X3)**	**MS/STD**
10.13	**45,73,100,147,192,218,266**	**phenylalanine**	**TMSi(X2)**	**MS/STD**
10.45	**45,73,116,188,231,292,333**	**Asparagine**	**TMSi(X3)**	**MS/STD**
10.56	**59,73,103,147,189,217,277,307**	**L-Arabinose**	**TMSi(X4)**	**MS/STD**
10.95	**59,73,86,130,174,214**	**Putrescine**	**TMSi(X4)**	**MS**
11.22	**45,73,100,128,156,203,245,273,301**	**Glutamine**	**TMSi(X3)**	**MS/STD**
11.52	**73,142,200,258,330**	**Ornithine**	**TMSi(X3)**	**MS/STD**
11.54	**45,73,157,217,256,330,373**	**Citrulline**	**TMSi(X4)**	**MS/STD**
11.55	**45,67,73,99,115,133,147,183,211,231**	**Citric acid**	**TMSi(X4)**	**MS/STD**

11.64	**73,100,146,174,199**	**Cadaverine**	**TMSi(X4)**	**MS**
12.16	**45,73,103,117,129,147,160,189,205,217,319**	**D-galactose**	**TMSi(X5)**	**MS/STD**
12.21	**59,73,86,128,156,200,230,317**	**Lysine**	**TMSi(X4)**	**MS/STD**
12.25	**45,59,73,82,100,132,147,154,166,218,238**	**Histidine**	**TMSi(X3)**	**MS/STD**
12.29	**59,73,103,147,205,319**	**D-glucose**	**TMSi(X5)**	**MS/STD**
12.35	**45,73,100,147,179,218,280**	**Tyrosine**	**TMSi(X3)**	**MS/STD**
12.38	**45,73,103,130,158,190,217,247**	**Pyruvic acid**	**TMSi(X2)**	**MS/STD**
12.93	**55,75,95,117,129,159,201,313**	**Palmitic acid(16:0)**	**TMSi(X1)**	**MS/STD**
13.40	**59,73,103,147,191,217,265,305**	**Myo-inositol**	**TMSi(X6)**	**MS/STD**
13.53	**55,75,95,117,132,159,201,327**	**Margaric acid(17:0)**	**TMSi(X1)**	**MS/STD**
13.56	**59,73,84,99,147,171,238,264,352**	**Guanine**	**TMSi(X3)**	**MS/STD**
13.95	**55,75,95,129,150,17,220,262,337**	**Linoleic acid(18:2)**	**TMSi(X1)**	**MS/STD**
14.01	**55,75,96,117,145,171,199,222,264,339**	**Oleic acid(18:1)**	**TMSi(X1)**	**MS/STD**
14.11	**55,75,95,117,129,159,201,341**	**Stearic acid(18:0)**	**TMSi(X1)**	**MS/STD**
14.13	**45,73,100,147,202,248,291,377,405**	**Tryptophan**	**TMSi(X3)**	**MS/STD**
14.71	**59,73,103,147,191,217,315,357,387**	**D-Fru-6-P**	**TMSi(X6)**	**MS/STD**
14.79	**59,73,101,147,191,217,247,299,357,387**	**D-Glc-6-p**	**TMSi(X6)**	**MS/STD**
15.20	**55,73,97,117,145,159,201,313,341**	**Arachidic acid(20:0)**	**TMSi(X1)**	**MS/STD**
15.40	**45,73,103,147,169,196,217,245,258,315**	**Uridine**	**TMSi(X4)**	**MS/STD**
15.69	**45,59,73,87,129,147,211,243,299,315,357**	**GlcNAc-6-P**	**TMSi(X7)**	**MS/STD**
16.05	**45,59,73,84,103,147,169,193,217,245,281**	**Inosine**	**TMSi(X4)**	**MS/STD**
16.13	**59,73,89,117,147,173,217,299,357,387**	**ManNAc-6-P**	**TMSi(X6)**	**MS/STD**
17.03	**45,73,103,147,189,217,245,280,324,368**	**Guanosine**	**TMSi(X5)**	**MS**
19.33	**73,95,119,129,145,213,255,275,329,368**	**Cholesterol**	**TMSi(X1)**	**MS/STD**

[a]Retention time.

[b]m/z values are the selected ions for identification and quantification of individual derivatized metabolies.

[c]Identified metabolites depended on variable importance projection (VIP) value under 0.7 and a p value <0.05.

[d]TMSi means trimethylsilyl.

[e]Identification: MS, mass spectrum was consistent with those of nist and in-house libraries; STD, mass spectrum was consistent with that of standard compound.

\

Sialic acid metabolism pathway analysis.

Mucin has polypeptide backbone with glycosylated carbohydrates (McGuckin et al., 2011), sialic acid is representative carbohydrate in the mucin. *nanA* which is the important gene related with metabolizing sialic acid was well-known virulence factor of *V. vulnificus* (Jeong *et al*., 2009). As shown in the Fig. 5, the genes related with sialic acid metabolism including *nanA* were highly induced, at least 6.48 fold to maximum 71.6 fold, in the *V. vulnificus* grown in the M9M (Jang *et al*., unpublished). Also, ManNAc-6-P and GlcNAc-6-P which were intermediates of sialic acid pathway were highly detected in the *V. vulnificus* grown in the mucin by metabolomics result.

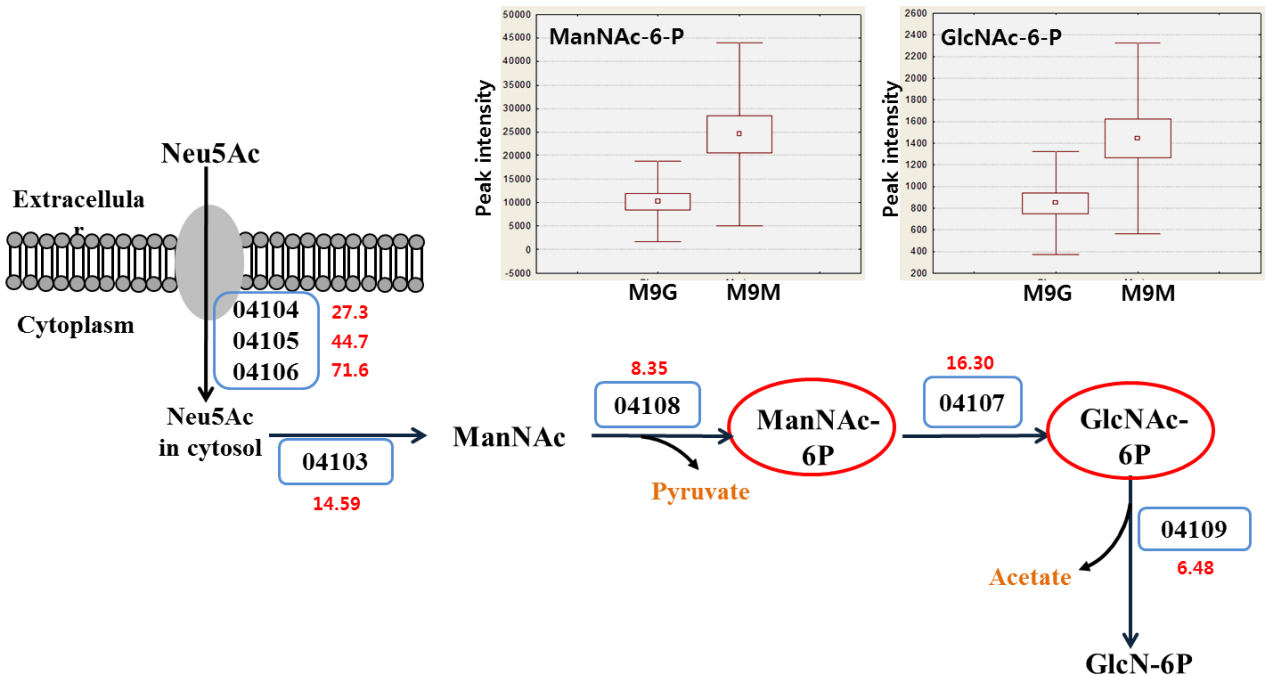

Fig. 5. Metabolic pathway of sialic acid (Neu5Ac) in *V. vulnificus* and box-whisker plots. A number in the blue box mean locus tag number of *V. vulnificus* and red numbers indicate a fold change of gene expression in M9M compared to M9G in the transcriptomic analysis (Jang *et al.*, unpublished). Two Box-whisker plots represent that ManNAc-6-P and GlcNAc-6-P were highly detected in the *V. vulnificus* grown in the mucin. (Neu5Ac, N-Acetylneuraminic acid; ManNAc, N-Acetyl-D-mannosamine; ManNAc-6-P, N-Acetyl-D-mannosamine-6-phosphate; GlcNAC-6-P, N-Acetylglucosamine-6-phosphate)

Construction of the mucin-secreting HT29-MTX cells and microscopic analysis for confirmations.

Most cells of HT-29 cultures are undifferentiated cells and small proportion of HT-29 culture is differentiated mucus-secreting cells (Huet *et al*., 1995). To obtain stably differentiated mucus-secreting cells, HT-29 cells were adapted to 10^{-6} M methotrexate (MTX) (Lesuffleur *et al*., 1990).

By using transmission electron microscopy (TEM), scanning electron microscopy (SEM) and confocal laser scanning microscope (CLSM), it was confirmed that constructed HT29-MTX cells produced and secreted the mucin.

As shown in Fig. 6 A, mucin granules were observed at postconfluent HT29-MTX cell in contrast with HT-29 cell. Also, HT29-MTX cell surface was covered with secreted mucin as shown in Fig. 6 B and C. (Gouyer *et al*., 2001). These results suggested that HT29-MTX cells are overlaid with secreted, gel-forming mucin.

A

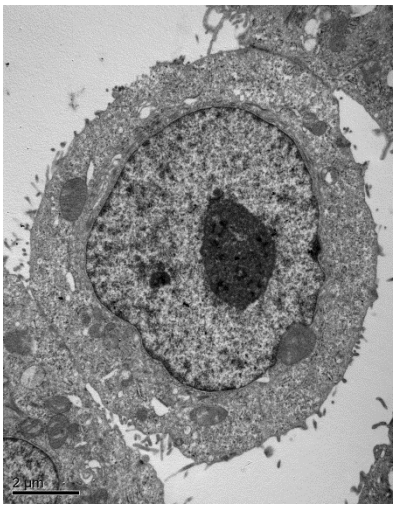

HT-29 cell

HT29-MTX cell

B

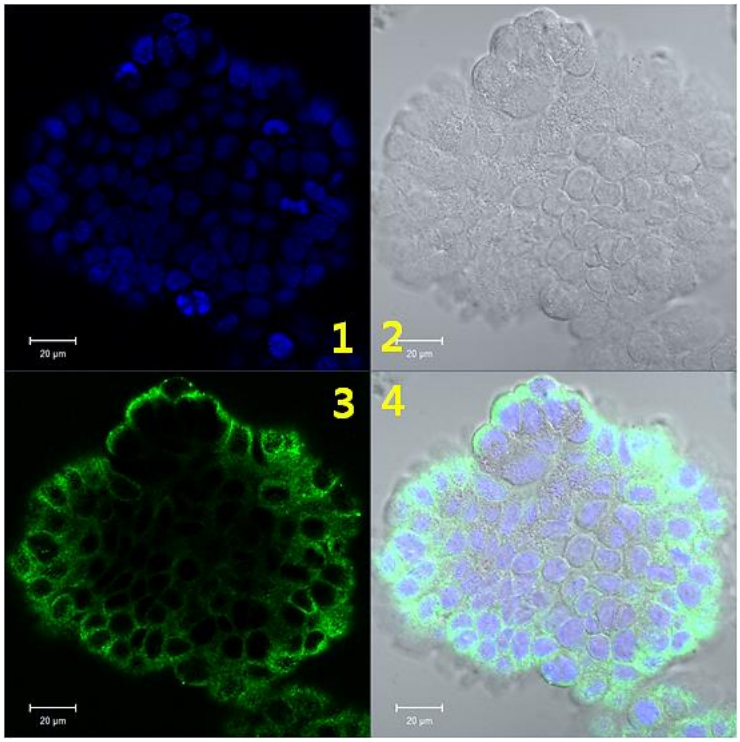

C

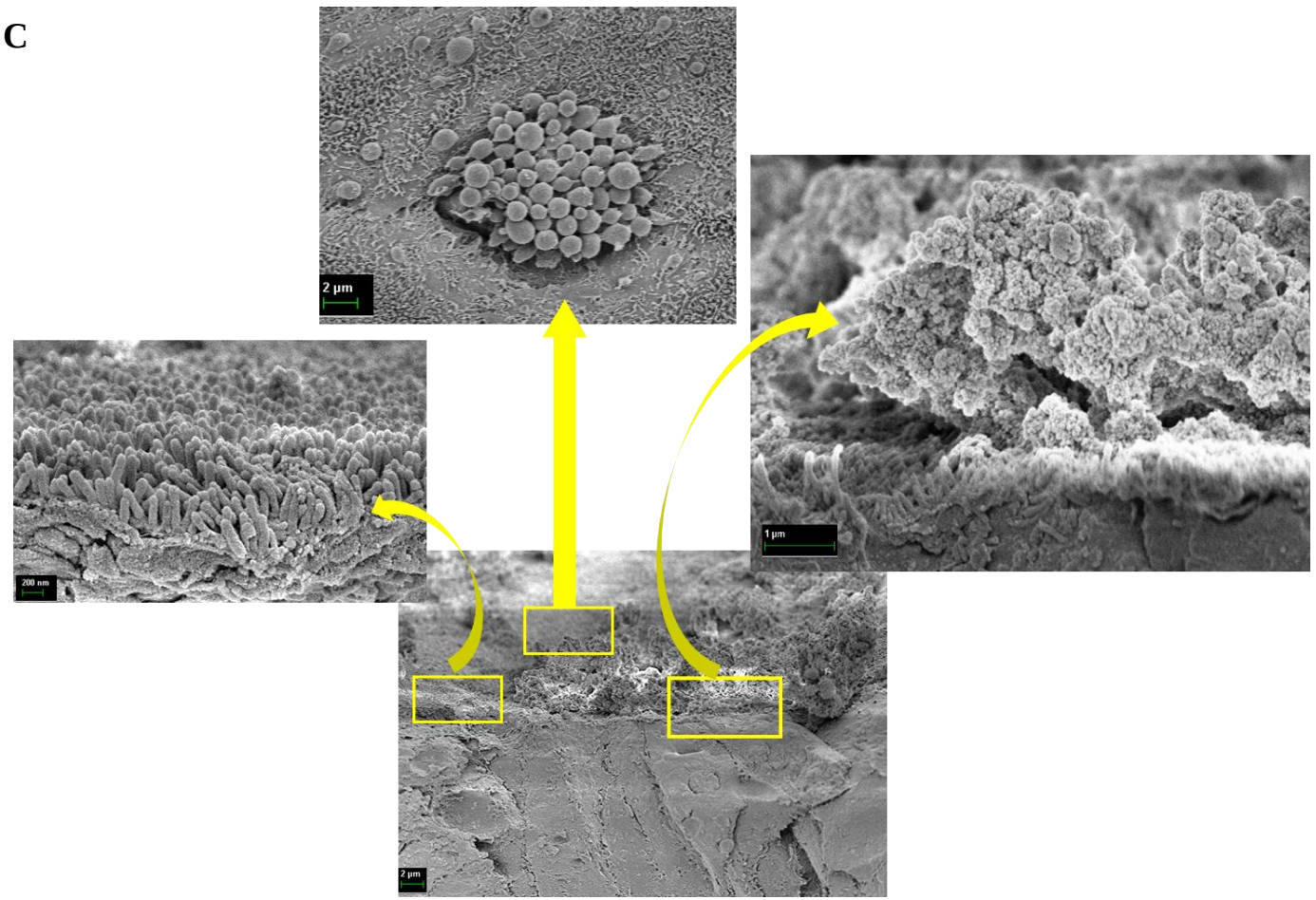

Fig. 6. Microscopic analysis of secreted gel-forming mucin by HT29-MTX cell line. (A) Transmission electron microscopy (TEM) of fluent cultures (day 10) of HT-29 and HT29-MTX. HT-29 cells didn't contain any mucin granules whereas HT29-MTX cells showed the exclusive presence of mucin granules. (B) Whole mount immunofluroscence staining analysis of secretion of MUC5AC mucin in preconfluent HT29-MTX cells (day 6). Nucleus was stained with DAPI as blue (image 1), and FITC conjugated antibody against secreted MUC5AC mucin was stained as green (image 3). Image2 is optical image of HT29-MTX cell and merged image of 1, 2, and 3 was presented as image 4. Confocal laser scanning microscope (CLSM) was used to visualize the images. (C) Scanning electron microscopy (SEM) of the cultured HT29-MTX cells (day 30) showing the brush border, budding mucus and mucus gel at the cell surface (left to right).

Survival assay of *V. vulnificus* infecting HT29-MTX cell line.

To explore the survival profile of *V. vulnificus* when infected in the mucin secreting cell line, HT29-MTX, survival assay was conducted. HT29-MTX cells were seeded in under part of polycarbonate membrane transwell culture plate. *V. vulnificus* were infected to outer part of insert. After incubation for infection, *V. vulnificus* which were in inner part of insert were collected for separation from detached eukaryotic cells.

As shown in the Fig. 7, *V. vulnificus* could survive and grow in the infecting condition in the HT29-MTX cell line and also in the BME medium for control.

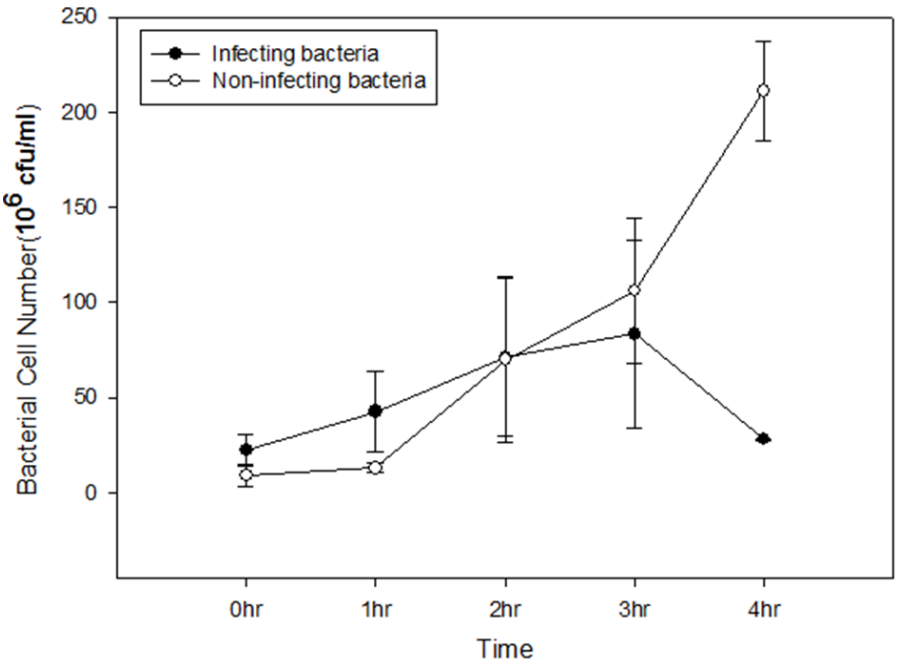

Fig. 7. Survival curve of *V. vulnificus* infecting HT29-MTX. Determination of *V. vulnificus* CFU(colony forming unit) infected with mucin-secreting HT29-MTX cells and BME medium control. CFU was determined by serial dilution method.

Schematic flow of sampling procedures of fast filtration.

Cold methanol quenching has been widely reported to cause serious cell leakage or cold shock, thus resulting in the loss of metabolites from both Gram-positive and negative bacteria and yeast. As an alternative to cold methanol quenching, fast filtration with direct extraction has been developed to reduce metabolite loss. Fast filtration with sampling times of several seconds prior to extraction appears to be a suitable approach for metabolites with relatively high intracellular level and low turnover such as amino acids or TCA cycle intermediates (Bolten et al., 2008). The Schematic flow diagram of fast filtration method using in this experiment was described in the Fig. 8.

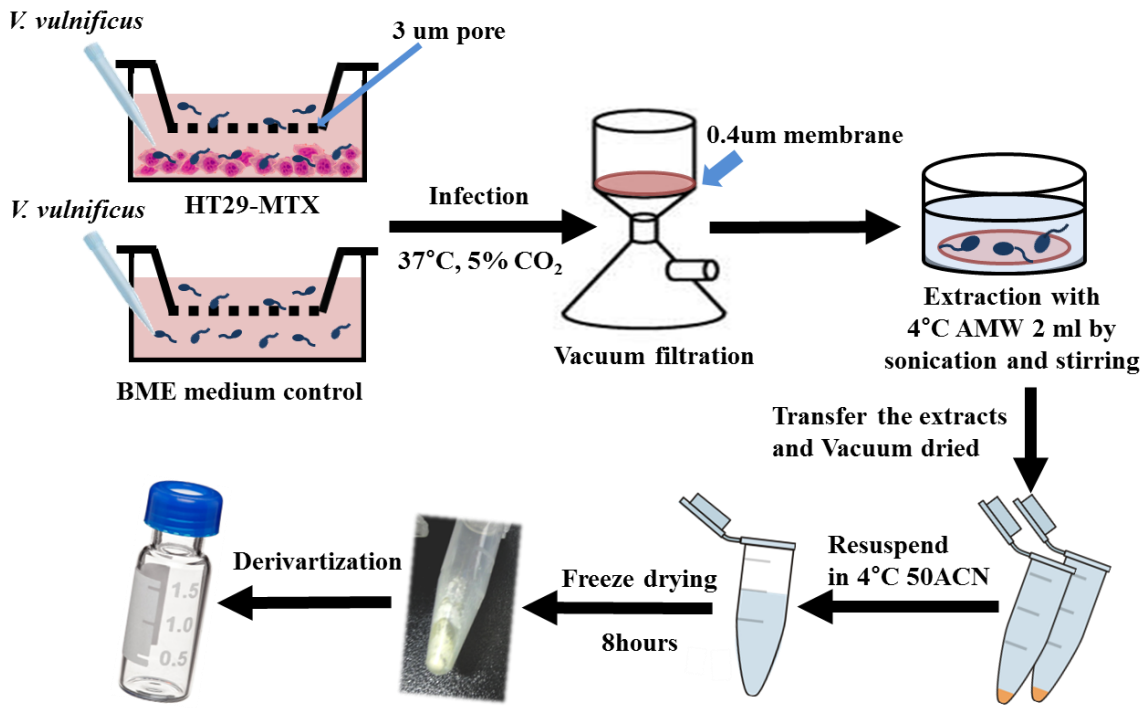

Fig. 8. Schematic flow of *ex vivo* sample preparation. The infecting *V.vulnificus* were vacuum fast filterated following washing were conducted by 10 ml of 0.9% NaCl. Then the cells attached membrane was quickly mixed with 2 ml of a metabolite extraction solvent the 4℃ mixture of AMW. Extraction was performed by sonication and stirring. The extracts were resuspended in fresh 50ACN at 4 ℃.

***Ex vivo*, multivariate analysis of metabolites profiles.**

A total of 12 samples from 6 different classes in two biological replicates and two analytical replicates were analyzed during the 1, 2, 3 hours infection. Metabolites from all major pathways, including lipids, sugars, and amino acids were detected. To provide comparative interpretations of the changes in metabolic profiles, partial least squares discriminant analysis (PLS-DA) for supervised evaluation (independent t-tests) were used to evaluate the mass spectral data of the metabolome from *V. vulnificus* infecting to mucin secreting HT29-MTX cell line and medium control.

In the PLS-DA analysis, vectors t[1] and t[2] explained 13.1% and 6.4% of the variation between *V. vulnificus* infecting to mucin secreting HT29-MTX cell line and medium control samples (Fig. 3 B). PLS-DA analysis revealed a clear separation of *V. vulnificus* metabolites between control and infecting.

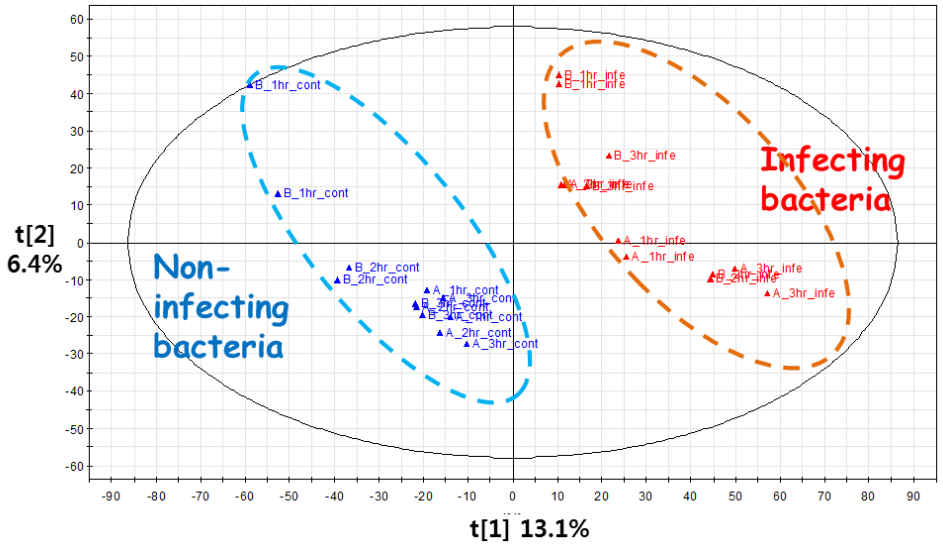

Fig. 9. *Ex vivo* analysis PLS-DA score plot. This plot was derived from GC-TOF-MS data sets analyzing *V. vulnificus* metabolism infecting to mucin secreting HT29-MTX cell line and medium control. This plot explained that the result of *V. vulnificus* metabolism infecting to mucin secreting HT29-MTX cell line is different from the metabolism in the grown in the medium control.

Comparison of metabolites abundances on the infecting *V. vulnificus*.

The metabolites reflecting variation between the *V. vulnificus* infecting mucin secreting HT29-MTX cell line and growing in medium control were identified based on the VIP and *p*-values. The identified metabolites were annotated based on their retention time in comparison with standards and their mass fragmentation (Table 3). A total of 16 primary metabolites, including 3 lipid-related compounds, 1 amine related compounds, 8 amino acids, 3 sugars and 1 organic acids showed significant variation among the samples (Fig. 10).

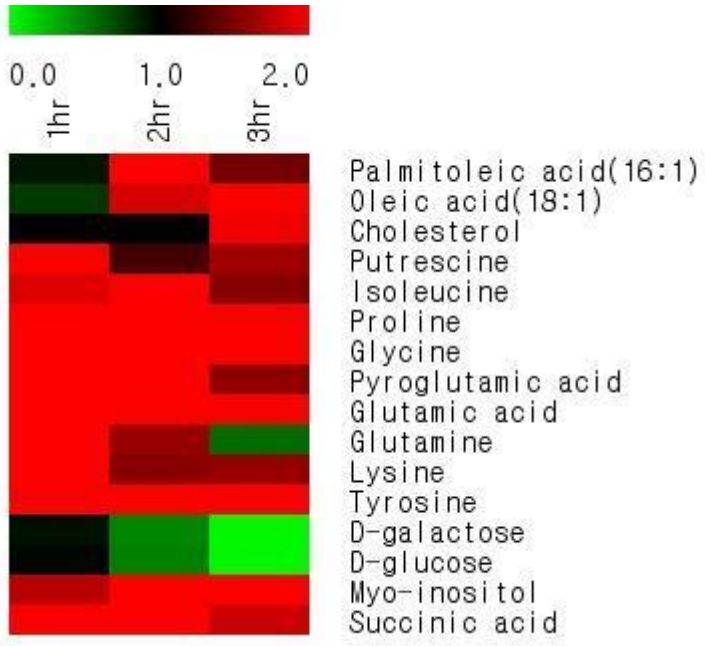

Fig. 10. Clustered heat map of *ex vivo* analysis. Significantly different intracellular metabolites between *V. vulnificus* infecting mucin secreting HT29-MTX cell line and growing in medium control. The number stands for the fold change ratio of infecting condition : :medium control (Variable selection: VIP value >0.7 and *p*-value <0.05).

Table 3. The most significantly different metabolites identified in the *V. vulnificus* infecting mucin secreting HT29-MTX cell line relative to growing in medium control.

RT[a](min)	MS fragmentation[b] (m/z)	Compound[c]	Derivatized[d]	ID[e]
7.26	**45,73,100,158,218,260,318,374**	**Isoleucine**	**TMSi(X2)**	**MS/STD**
7.30	**45,59,73,84,100,133,142,216**	**Proline**	**TMSi(X2)**	**MS/STD**
7.39	**45,73,86,117,147,174,248,276,357**	**Glycine**	**TMSi(X3)**	**MS/STD**
7.41	**45,55,73,86,129,147,172,218,247**	**Succinic acid**	**TMSi(X2)**	**MS/STD**
9.29	**45,73,147,156,157,230,258**	**Pyroglutamic acid**	**TMSi(X2)**	**MS/STD**
10.02	**45,73,100,128,174,204,246,274,320**	**Glutamic acid**	**TMSi(X3)**	**MS/STD**
10.95	**59,73,86,130,174,214**	**Putrescine**	**TMSi(X4)**	**MS**
11.22	**45,73,100,128,156,203,245,273,301**	**Glutamine**	**TMSi(X3)**	**MS/STD**
12.16	**45,73,103,117,129,147,160,189,205,217,319**	**D-galactose**	**TMSi(X5)**	**MS/STD**
12.21	**59,73,86,128,156,200,230,317**	**Lysine**	**TMSi(X4)**	**MS/STD**
12.29	**59,73,103,147,205,319**	**D-glucose**	**TMSi(X5)**	**MS/STD**
12.35	**45,73,100,147,179,218,280**	**Tyrosine**	**TMSi(X3)**	**MS/STD**
12.80	**41,43,55,67,69,73,75,96,117,129,145,339**	**Palmitoleic acid**	**TMSi(X1)**	**MS**
13.40	**59,73,103,147,191,217,265,305**	**Myo-inositol**	**TMSi(X6)**	**MS/STD**
14.01	**55,75,96,117,145,171,199,222,264,339**	**Oleic acid(18:1)**	**TMSi(X1)**	**MS/STD**
19.33	**73,95,119,129,145,213,255,275,329,368**	**Cholesterol**	**TMSi(X1)**	**MS/STD**

[a]Retention time.

[b]m/z values are the selected ions for identification and quantification of individual derivatized metabolies.

[c]Identified metabolites depended on variable importance projection (VIP) value under 0.7 and a p value <0.05.

[d]TMSi means trimethylsilyl.

[e]Identification: MS, mass spectrum was consistent with those of nist and in-house libraries; STD, mass spectrum was consistent with that of standard compound.

Analysis of fatty acid metabolism pathway in *V. vulnificus*

Fatty acid related compounds were more detected in *V. vulnificus* grown in the mucin medium and in the infecting bacteria sample. The mucin powder supplemented to the medium is commercialized porcine stomach mucin. Thus, there was possibility to porcine cell membrane component in the powder. It could give lipid sources for *V. vulnificus.* Also mucus component in the HT29-MTX cells such as phospholipid, cholesterol, several fatty acids can also be utilized by *V. vulnificus*.

In the fatty acid metabolic pathway, cytoplasmic fatty acid is degraded by beta oxidation. During beta oxidation, cofactors such as Acetyl CoA, $FADH_2$, and NADH are concentrated in cytosol and these are related ATP production.

As shown in the Fig. 11 A and B, when *V. vulnificus* utilized mucin through the supplemented in the medium or secreted from the cell line, the fatty acid degradation and biosynthesis related gene expressions were increased (Jang *et al*., unpublished). Also, in the metabolomics approach, several fatty acids were highly metabolized especially one of the unsaturated fatty acid, oleic acid, was highly detected both *in vitro* and *ex vivo* experiment. Consist with this; the gene *fab*A which encodes 3-hydroxydecanoyl-[acyl-carrier-protein] dehydratase and influences to form unsaturated fatty acid (Cronan and Thomas. 2009; Feng and Cronan. 2009) was highly induced in the transcriptomic analysis (Fig. 11 B).

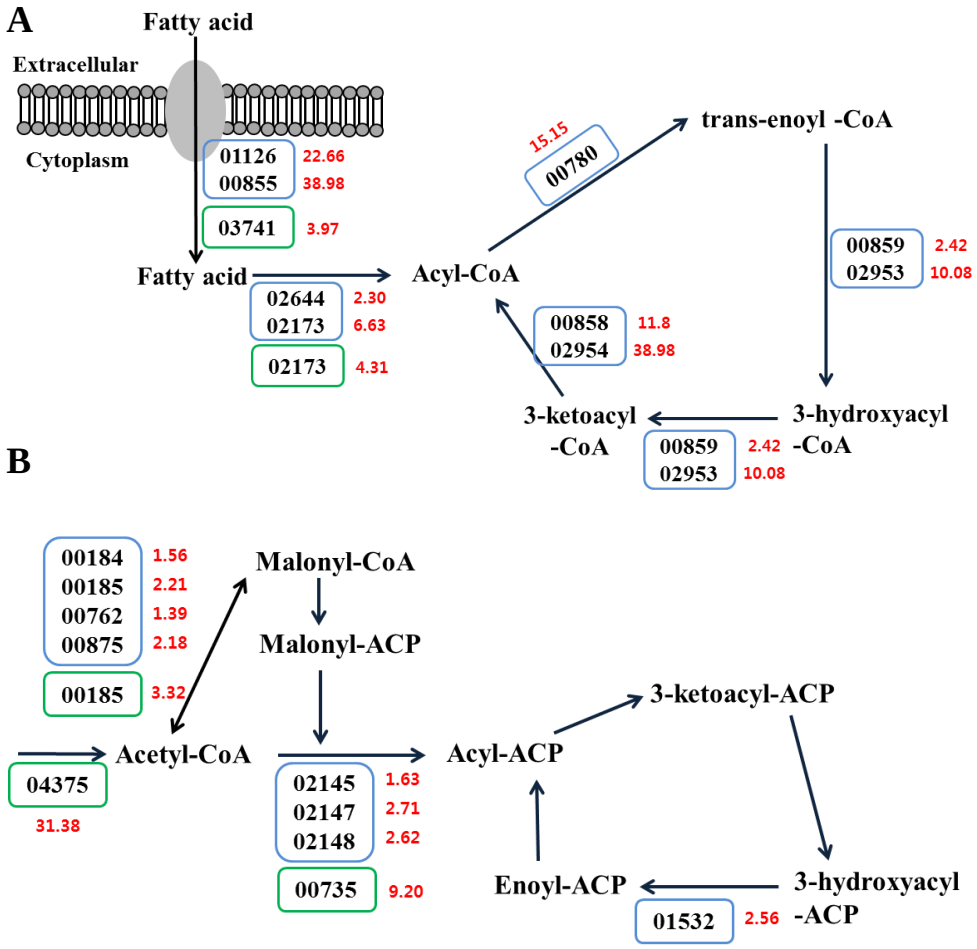

Fig. 11. Metabolic pathway of fatty acid in *V. vulnificus*. (A) Fatty acid degradation pathway in *V. vulnificus* and (B) Fatty acid biosynthesis pathway in *V. vulnificus*. A number in the square box is locus tag number of *V. vulnificus* (Blue: gene expressed in the *in vitro* experiment; Green: gene expressed in the *ex vivo* experiment) and red numbers indicate a fold change of gene expression by mucin and infection (Jang *et al.*, unpublished).

IV. DISCUSSION

Vibrio vulnificus is a Gram-negative marine bacterium that is known as a significant opportunistic human pathogen. *V. vulnificus* mediated food-borne diseases are normally occurred by ingestion of the contaminated oyster and seafood. Typically, *V. vulnificus* entered the small intestine and invades the bloodstream causing severe septicemia (Gulig *et al*., 2005).

The extracellular secreted mucus and the cell surface glycocalyx prevent infection by the vast numbers of microorganisms that live in the healthy gut. Mucin glycoproteins are the major component of these barriers. However, successful enteric pathogens have evolved strategies to circumvent these barriers (McGuckin *et al.*, 2011). The mucous layer contains mucins that are highly glycosylated polymorphic glycoproteins and composes with water, salts, lipid related compounds (Allen, 1981). To be a successful pathogen, *V. vulnificus* must be able to use nutrients existed in the intestinal mucus layer. Mucin utilizing by *V. vulnificus* must be important step for the first stage of infection. Therefore, it is very significant to understand the *V. vulnificus* metabolism when they utilize mucin as a nutrient. I tried to provide insight into mucin utilization of *V. vulnificus* in order to find out control target for *V. vulnificus* initial stage of infection.

The metabolome is much more sensitive to perturbations in the environment than either the transcriptome or the proteome because the metabolites within a cell are an integrated reflection of the cellular phenotype (Sellick *et al*., 2009). However, different from the other 'omics', metabolomics includes methodological problems derived from heterogeneity in chemical properties (Ohashi *et al*., 2008). In this reason, metabolome sampling is one of the most important factors determine the quality of metabolomics data (Kim et al., 2013). Here, I used cold methanol quenching method for *in vitro* experiment (Fig. 2) and fast filtration method for *ex vivo* experiment (Fig. 8) respectively. Even though when cold methanol quenching was applied, serious losses of intracellular metabolites due to cell leakage were observed in bacteria (Shin *et al*., 2010b), still this method is widely used for Gram-negative and Gram-positive bacterial quenching. In bacteria, as an alternative to cold methanol quenching, the fast filtration method was developed and shown to be effective in minimizing the losses of intracellular metabolites both in Gram-negative and Gram-positive bacteria (Bolten *et al*., 2007). In the case of *in vitro* experiment, mucin polymer stuck the membrane filter that hindered the filtration thus that experiment was conducted by cold methanol quenching.

From the *in vitro* experiment, it was verified that *V. vulnificus* survived and grew using porcine gastric mucin as the sole source of nutrient (Fig. 1). Also, the principal component analysis revealed clear separations between the metabolite profiles of cells grown with mucin and glucose (Fig. 3). The discriminative metabolites between each conditions were 13 lipid related compounds, 8 amine

related compounds, 17 amino acids, 8 sugars and 4 organic acids (Fig. 4). Glycolysis intermediates such as glucose-6-p and fructose-6-p were decreased in the cells grown with mucin. However, most of metabolites were highly detected in the *V. vulnificus* metabolized mucin. Especially, silaic acid (Neu5Ac) pathway intermediates such as ManNAc-6-P and GlcNAc-6-P were more detected (Fig. 5). N-acetylneuraminate lyase (NanA) initiates the catabolism of Neu5Ac by cleaving it into pyruvate and N-acetylmannosamine (ManNAc) in most bacteria (Almagro-Moreno and Boyd, 2009). The *nanA* mutant was defective for intestinal colonization and significantly diminished in virulence in a mouse model (Jeong *et al*., 2009). These results suggested that the catabolic utilization of Neu5Ac is essential for the pathogenesis of the bacteria by ensuring growth and survival during infection. Therefore, this pathway related genes might be the important control target to *V. vulnificus* initial infection.

In the experiment of *ex vivo*, *V. vulnificus* survival and growth ability when infected to mucin secreting human carcinoma HT29-MTX cell line were confirmed (Fig. 7). It was known theat the interactions between enteric pathogens and mucins, and the mechanisms that these pathogens use to disrupt and avoid mucosal barriers (McGuckin *et al*., 2011). In addition to the principal component analysis showed clear separations between the metabolites between *V. vulnificus* infecting HT29-MTX which means mucin metabolized bacteria and medium control (Fig. 9). The discriminative metabolites between each conditions were including 3 lipid related

compounds, 1 amine related compounds, 8 amino acids, 3 sugars and 1 organic acids (Fig. 10).

Analysis of both experiment collectively, the amounts of amino acids, fatty acids and TCA cycle intermediates were increased in *V. vulnificus* grown with mucin and infecting *V. vulnificus*. These suggest that *V. vulnificus* preferentially activates the catabolisms of amino acids and fatty acids to produce TCA cycle intermediates in the utilization of mucin. The major fatty acid species existing in the *V. vulnificus* are palmitic acid (16:0), palmitoleic acid (16:1), oleic acid (18:1). Those fatty acids increased in the result from mucin metabolism. The primary role of bacterial fatty acid is to act as the hydrophobic component of the membrane lipids and as components of storage lipids (Cronan and Thomas. 2009). The envelope plays a crucial role in facilitating response to environmental changes (Linder and Oliver. 1989). In this aspects, increased amounts of fatty acid by metabolizing mucin means important factors to stabilize cell membrane for *V. vulnificus*.

If we can prevent the metabolic pathway related to mucin utilization, we can control the *V. vulnificus* initial stage of infection. This study is expected to give important clues in understanding the initial infection stage of *V. vulnificus* metabolism by using mucin. However, it should be additionally studied deeper pathway analysis about each metabolites highly detected in the mucin utilizing *V. vulnificus*. Also, it would be better to try systematical interpretation with transcriptomic analysis in

order to figure out more concise understanding of the state of *V. vulnificus* at initial infection stage.

V. REFERNCES

Allen A. (1981). Structure and function of gastrointestinal mucus. In: Johnson L, editor. Physiology of the gastroenterology tract, 1st edition. New York, NY' Raven Press, 617– 39.

Almagro-Moreno, S. & Boyd, E. F. (2009). Insights into the evolution of sialic acid catabolism among bacteria. *BMC Evolutionary Biology* **9**, 118.

Benitez, J., Spelbrink, R., Silva, A., Phillips, T., Stanley, C., Boesman-Finkelstein, M. & Finkelstein, R. (1997). Adherence of Vibrio cholerae to cultured differentiated human intestinal cells: an in vitro colonization model. *Infection and immunity* **65**, 3474-3477.

Bolten, C. J., Kiefer, P., Letisse, F., Portais, J.-C. & Wittmann, C. (2007). Sampling for metabolome analysis of microorganisms. *Analytical chemistry* **79**, 3843-3849.

Brown, S. A., Palmer, K. L. & Whiteley, M. (2008). Revisiting the host as a growth medium. *Nature Reviews Microbiology* **6**, 657-666.

Buchholz, A., Hurlebaus, J., Wandrey, C. & Takors, R. (2002). Metabolomics: quantification of intracellular metabolite dynamics. *Biomolecular engineering* **19**, 5-15.

Chang, D.-E., Smalley, D. J., Tucker, D. L. & other authors (2004). Carbon nutrition of Escherichia coli in the mouse intestine. *Proceedings of the National Academy of Sciences of the United States of America* **101**, 7427-7432.

Cronan, J. E. & Thomas, J. (2009). Bacterial fatty acid synthesis and its relationships with polyketide synthetic pathways. *Methods in enzymology* **459**, 395-433.

Dunn, W. B. & Ellis, D. I. (2005). Metabolomics: current analytical platforms and methodologies. *TrAC Trends in Analytical Chemistry* **24**, 285-294.

Donelli, G., Fabbri, A. & Fiorentini, C. (1996). Bacteroides fragilis enterotoxin induces cytoskeletal changes and surface blebbing in HT-29 cells. *Infection and immunity* **64**, 113-119.

Feng, Y. & Cronan, J. E. (2009). Escherichia coli unsaturated fatty acid synthesis complex transcription of the fabA gene and in vivo identification of the essential

reaction catalyzed by FabB. *Journal of Biological Chemistry* **284**, 29526-29535.

Fiehn, O. (2002). Metabolomics–the link between genotypes and phenotypes. *Plant molecular biology* **48**, 155-171.

Gulig, P. A., Bourdage, K. L. & Starks, A. M. (2004). Molecular Pathogenesis of *Vibrio vulnificus*. *J. Micobiol.* **43**, 118-131

Gouyer, V., Wiede, A., Buisine, M.-P., Dekeyser, S., Moreau, O., Lesuffleur, T., Hoffmann, W. & Huet, G. (2001). Specific secretion of gel-forming mucins and TFF peptides in HT-29 cells of mucin-secreting phenotype. *Biochimica et Biophysica Acta (BBA)-Molecular Cell Research* **1539**, 71-84.

Hellerstein, M. K. (2004). New stable isotope–mass spectrometric techniques for measuring fluxes through intact metabolic pathways in mammalian systems: introduction of moving pictures into functional genomics and biochemical phenotyping. *Metabolic engineering* **6**, 85-100.

Huet, G., Kim, I., De Bolos, C. & other authors (1995). Characterization of mucins and proteoglycans synthesized by a mucin-secreting HT-29 cell subpopulation. *Journal of cell science* **108**, 1275-1285.

Jeong, H. G., Oh, M. H., Kim, B. S., Lee, M. Y., Han, H. J. & Choi, S. H. (2009). The capability of catabolic utilization of N-acetylneuraminic acid, a sialic acid, is essential for Vibrio vulnificus pathogenesis. *Infection and immunity* **77**, 3209-3217.

Kim, S., Lee, D. Y., Wohlgemuth, G., Park, H. S., Fiehn, O. & Kim, K. H. (2013). Evaluation and optimization of metabolome sample preparation methods for Saccharomyces cerevisiae. *Analytical chemistry* **85**, 2169-2176.

Lång, H., Jonson, G., Holmgren, J. & Palva, E. T. (1994). The maltose regulon of Vibrio cholerae affects production and secretion of virulence factors. *Infection and immunity* **62**, 4781-4788.

Linkous, D. A. & Oliver, J. D. (1999). Pathogenesis of *Vibrio vulnificus*. *FEMS Microbiol Lett.* **174**, 207-214

Lesuffleur, T., Barbat, A., Dussaulx, E. & Zweibaum, A. (1990). Growth adaptation to methotrexate of HT-29 human colon carcinoma cells is associated with their ability to differentiate into columnar absorptive and mucus-secreting cells. *Cancer research* **50**, 6334-6343.

Marcinowska, R., Trygg, J., Wolf-Watz, H., Mortiz, T. & Surowiec, I. (2011). Optimization of a sample preparation method for the metabolomic analysis of clinically relevant bacteria. *Journal of microbiological methods* **87**, 24-31.

Mashego, M. R., Rumbold, K., De Mey, M., Vandamme, E., Soetaert, W. & Heijnen, J. J. (2007). Microbial metabolomics: past, present and future methodologies. *Biotechnology letters* **29**, 1-16.

Mitsui, Y., Matsumura, K., Kondo, C. & Takashima, R. (1976). The role of mucin on experimental Pseudomonas keratitis in rabbits. *Investigative Ophthalmology & Visual Science* **15**, 208-210.

McGuckin, M. A., Lindén, S. K., Sutton, P. & Florin, T. H. (2011). Mucin dynamics and enteric pathogens. *Nature Reviews Microbiology* **9**, 265-278.

Melissa, K. J. & Oliver, J. D. (2009). *Vibrio vulnificus*: Disease and Pathogenesis. *Infec. Immun.* **77**:1723-173

Ohashi, Y., Hirayama, A., Ishikawa, T., Nakamura, S., Shimizu, K., Ueno, Y., Tomita, M. & Soga, T. (2008). Depiction of metabolome changes in histidine-starved Escherichia coli by CE-TOFMS. *Molecular BioSystems* **4**, 135-147.

Pontier, C., Pachot, J., Botham, R., Lenfant, B. & Arnaud, P. (2001). HT29-MTX and Caco-2/TC7 monolayers as predictive models for human intestinal absorption: Role of the mucus layer. *Journal of pharmaceutical sciences* **90**, 1608-1619.

Pope, G. A., MacKenzie, D. A., Defernez, M. & other authors (2007). Metabolic footprinting as a tool for discriminating between brewing yeasts. *Yeast* **24**, 667-679.

Rose. M. C. (1992). Mucins: structure, function, and role in pulmonary diseases. *Lung Physio*l. **263**:L413-L429

Sambrook, J., and Russell, D. W. (2001). Molecular cloning: a laboratory menual, 3rd ed. Cold Spring Harbor Laboratory, Cold Spring Harbor, NY.

Scherling, C., Roscher, C., Giavalisco, P., Schulze, E.-D. & Weckwerth, W. (2010). Metabolomics unravel contrasting effects of biodiversity on the performance of individual plant species. *PloS one* **5**, e12569.

Sellick, C. A., Hansen, R., Maqsood, A. R., Dunn, W. B., Stephens, G. M., Goodacre, R. & Dickson, A. J. (2008). Effective quenching processes for physiologically valid metabolite profiling of suspension cultured mammalian cells. *Analytical chemistry* **81**, 174-183.

Shin, M. H., Lee, D. Y., Skogerson, K., Wohlgemuth, G., Choi, I. G., Fiehn, O. & Kim, K. H. (2010). Global metabolic profiling of plant cell wall polysaccharide degradation by Saccharophagus degradans. *Biotechnology and bioengineering* **105**,

477-488.

Shin, M. H., Lee do, Y., Wohlgemuth, G., Choi, I. G., Fiehn, O. & Kim, K. H. (2010a). Global metabolite profiling of agarose degradation by Saccharophagus degradans 2-40. *N Biotechnol* **27**, 156-168.

Shin, M. H., Lee, D. Y., Liu, K.-H., Fiehn, O. & Kim, K. H. (2010b). Evaluation of sampling and extraction methodologies for the global metabolic profiling of Saccharophagus degradans. *Analytical chemistry* **82**, 6660-6666.

Strom, M. S., & Paranjpye. R. N. (2000). Epidemiology and pathogenesis of *Vibrio vulnificus*. *Micobes Infect*. **2**:177-188

Van der Werf, M. J., Overkamp, K. M., Muilwijk, B., Koek, M. M., van der Werff-van, B. J., Jellema, R. H., Coulier, L. & Hankemeier, T. (2008). Comprehensive analysis of the metabolome of Pseudomonas putida S12 grown on different carbon sources. *Molecular BioSystems* **4**, 315-327.

Vieira, M. A., Gomes, T. A., Ferreira, A. J., Knöbl, T., Servin, A. L. & Liévin-Le Moal, V. (2010). Two atypical enteropathogenic Escherichia coli strains induce the production of secreted and membrane-bound mucins to benefit their own growth at the apical surface of human mucin-secreting intestinal HT29-MTX cells. *Infection and immunity* **78**, 927-938.

Villas-Bôas, S. G., Noel, S., Lane, G. A., Attwood, G. & Cookson, A. (2006). Extracellular metabolomics: a metabolic footprinting approach to assess fiber degradation in complex media. *Analytical biochemistry* **349**, 297-305.

VI. 국문초록

패혈증 비브리오균은 그람 음성의 운동성을 갖는 균으로서 해산물을 날것으로 섭취하거나 상처 부위가 바닷물에 노출되었을 경우 감염되게 된다. 감염 시, 심각한 위장염이나 패혈증을 유발하게 되며, 사망률이 50%가 넘는 것으로 알려져 있다. 뮤신은 글라이코실레이션 (glycosylation) 이 많이 되어있는 큰 분자량을 갖는 당단백질의 일종으로 인체 내의 점액층 (mucus layer)의 주요 성분이다. 점액층은 병원균을 막는 방어선 역할을 하며 또한 병원균의 성장을 돕는 영양원을 제공하게 된다. 패혈증 비브리오균의 뮤신 이용에 따른 대사체 변화를 분석함으로써, 패혈증 비브리오균의 초기 감염 시 특이적으로 증가하는 대사 경로를 GC-MS (가스 크로마토그래피-질량분석기)를 이용한 글로벌 분석을 통해 알아보았다. 시험관 수준에서 뮤신 파우더와 글루코스를 각각 첨가한 배지에 배양한 패혈증 비브리오균의 대사산물을 추출하고 다변량 통계 분석한 결과, 두 배지에서 자란 균에서 나온 대사체는 극명한 차이를 보임을 알 수 있었다. 또한 뮤신을 만들어 내는 세포주를 구축하고, 세포주와 배지 대조군에 패혈증 비브리오 균을 각각 감염시킨 후 비브리오 균의 대사체 변화를 분석하였다. 역시 다변량 통계 분석 결과 세포주가 만들어 낸 뮤신을 이용해 감염한 비브리오 균과 대조군 사이의 대사체에 차이가 있음을 확인하였다. 이렇게 뮤신을 이용했을 때

차이는 보이는 물질을 질량분석기 데이터 베이스와 표준물질의 크로마토그램 결과를 통해 확인한 결과, 다양한 지방산, 아미노산, TCA 회로의 중간 물질, 시알산 분해 경로의 중간 물질 등이 뮤신을 대사한 결과 증가함을 확인하였다. 이를 통해 초기감염 시, 패혈증 비브리오균이 뮤신을 이용하여 대사함을 확인하였고, 이를 통해 활성화 되는 대사경로 역시 알 수 있었다. 뮤신 이용 시 활성화되는 대사 경로를 비브리오 균을 제어하는 타겟으로 삼아, 비브리오 균의 초기감염을 막는 저해제를 찾을 수 있을 것이다.